



steel, the spacing of rectangular hoops and Young's modulus of concrete and steel are considered in this new model. The relations are given as follows:

$$\text{For } \sigma_c \text{ vs } \epsilon_{cp} : \sigma_c = f_c'' \left( \frac{2\sigma_c}{f_c''} \right)^2 \left( \frac{\epsilon_{cp}}{\epsilon_u} \right) \left( \frac{f_c''}{f_c'} \right)^2$$

$$\text{With: } f_c'' = 0.85 \left( \frac{s_d}{s_t} \right)^2 \sqrt{\frac{E_s}{E_c}} f_c'$$

$$\text{For } \epsilon_{cp} \text{ vs } \epsilon_u : \epsilon_{cp} = f_c'' \left( \frac{1}{z} \right) \left( \frac{\epsilon_{cp}}{\epsilon_u} \right)^2$$

$$\text{With: } z = \frac{0.5}{t_1 + t_2 + 0.002}$$

under condensed form, where:

$$t_1 = \frac{3 + 0.002 f_c'}{f_c' + 1000} \quad \text{and} \quad t_2 = 0.75 \left( \frac{b_t}{s_t} \right) \left( \frac{1}{b + d} \right) \sqrt{\frac{E_s s_d}{E_c s_t^2}}$$

In which:

- $\sigma_c, \epsilon_c$  : uniaxial stress and strain of concrete;
- $E_s, E_c$  : Young's elastic modulus of steel and concrete respectively;
- $f_c''$  : peak compressive stress of confined concrete;
- $\epsilon_{cp}$  : strain at peak compressive stress  $f_c'$ ;
- $\epsilon_u$  : maximum strain;
- $\epsilon_t$  : ratio of volume of transverse reinforcement to volume of concrete core measured to outside of hoops;
- $s_d$  : summation of diameters of longitudinal reinforcement;
- $s_t$  : spacing of hoops;
- $z$  : Parameter defining the slope of the linear descending branch of the compressive stress-strain curve of concrete;
- $b_t$  : width of concrete core measured to outside of hoops;
- $b, d$  : dimensions of cross section of beam element;

### Tension stiffening

It is assumed that the concrete will carry some tensile stresses when it reaches its ultimate tensile strength. This approach has been used by many authors [14,15]. A bilinear stress-strain curve is adopted, with a linear ascending branch and a linear softening branch for concrete after cracking (fig. 1).

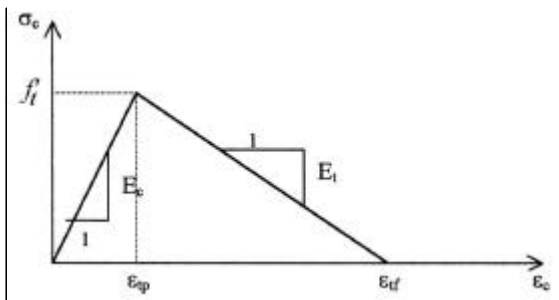


Figure 1: Bilinear stress-strain relation for concrete in tension.

This behaviour may be characterised as follows:

$$\text{For } \sigma_c \text{ vs } \epsilon_{tp} : \sigma_c = E_c \epsilon_c$$

$$\text{For } \epsilon_{tp} \text{ vs } \epsilon_{tf} : \sigma_c = f_t' \left( \frac{\epsilon_c - \epsilon_{tp}}{\epsilon_{tf} - \epsilon_{tp}} \right) E_t$$

$$\text{For } \sigma_c \text{ vs } \epsilon_{tf} : \sigma_c = 0$$

In which :

$f_t'$  : direct tensile strength;

$E_t$  : tangent strain-softening modulus;

$\epsilon_{tp}$  : strain at peak tensile stress;

$\epsilon_{tf}$  : final strain when the tensile stress is reduced to zero.

### Steel reinforcement

The steel is assumed as elastic perfectly plastic, characterised by Young's elastic modulus  $E_s$  and uniaxial yield stress  $f_y$ .

### FINITE ELEMENT ANALYSIS

A reinforced concrete beam is divided into many dimensional beam elements. Each element is assumed to have three degrees of freedom. Its rectangular section is divided into a discrete number of layers in the direction perpendicular to the axis of symmetry. The geometry of each layer is defined by its length, width and the distance between its mid-height and the reference axis  $y_j$  (fig. 2). In each cross section the stiffness matrix is obtained by summation of similar matrices of each layer.

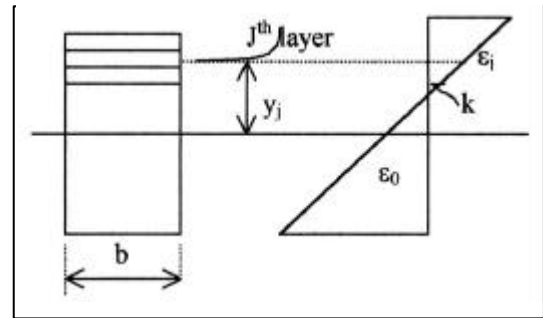


Figure 2 Layered model and strain distribution for concrete section.

The usual Bernoulli-Navier's hypothesis that a plane cross sections of the beam remain plane and orthogonal is adopted. Further, it is assumed that the average strain in steel equals the average strain in concrete at the same level. The linearity of strain distribution requires that  $\epsilon_j = \epsilon_0 + k y_j$ .

Where:

$\epsilon_j$  : strain at  $j^{\text{th}}$  layer,

$\epsilon_0$  strain at axis reference,

$k$  : curvature,

$y_j$ : distance between reference axis and the mid-height of layer  $j$ .

The stiffness matrix elements are given as follows:

$$D = \begin{bmatrix} EA & EM \\ EM & EI \end{bmatrix}$$

Where:

$EA$  : secant axial stiffness,

$EI$  : secant flexure stiffness,

$EM$  : secant coupling stiffness,

$$EA = \sum_{j=1}^{nc} E_j A_j + \sum_{j=1}^{ns} E_j A_{sj}$$

$$EI = \sum_{j=1}^{nc} E_j Y_j^2 A_j + \sum_{j=1}^{ns} E_j Y_j^2 A_{sj}$$

$$EM = \sum_{j=1}^{nc} E_j Y_j A_j + \sum_{j=1}^{ns} E_j Y_j A_{sj}$$

Where:

$n_c, n_s$ : Number of concrete layers and steel layers in a cross section respectively;

$E_j$  : Young's modulus of elasticity of layer  $j$  ;

$A_j$  : Area of concrete layer  $j$ .

$A_{sj}$  : Area of steel layer  $j$

## NON-LINEAR SOLUTION PROCEDURE

A Newton-Raphson non-linear method is adopted in which the secant stiffness matrices are updated at the beginning of each iteration. The convergence criterion used in this study is the one used by Ahmed and *al.* [16]. The iterative cycles are repeated until the convergence. The convergence is reached when the differences between the axial strain at the reference axis ( $\epsilon_0$ ) and the curvature ( $\epsilon'$ ) determined in two successive cycles are smaller than a certain tolerance, and then the load is incremented.

The convergence criterion is defined by the following relations:

$$\epsilon_0 - \epsilon_0' \leq \frac{du}{dx}$$

$$\epsilon' - \epsilon' \leq \frac{\epsilon' \epsilon_0}{L}$$

Where:

$\epsilon_i, \epsilon_j$ : are the rotations in nodes  $i$  and  $j$  respectively,

$L$ : element length.

## Determination of the maximum load and analysis of the descending branch of stress-strain curve

During the iterative procedure, if the maximum load is exceeded, the convergence will not take place and the maximum number of iterations is reached. Each time this number is reached, the program goes back to the previous loading and changes the load increment once again to half the increment step. When the value of the step ( $\Delta p_i$ ) becomes smaller than a certain tolerance, the program gives the maximum load (fig. 3).

The determined maximum load corresponds to the peak of stress – strain curve. The coordinates of this point will be useful for the analysis of the descending branch of this curve.

Once the peak is determined, the program changes the coordinate system in order to be able to analyse the descending branch of the stress – strain curve. The change of coordinate system is illustrated in figure 3. The descending branch of the curve, in the coordinate system ( $\sigma_c - \epsilon_c$ ), becomes an ascending one, in the coordinate system ( $\sigma_c' - \epsilon_c'$ ).

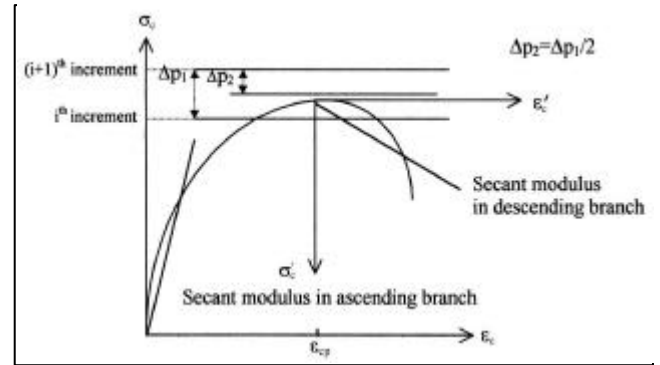


**Figure 3** Representation of the change of axis at the peak in stress-strain curve.

## Comparison with test data

Two numerical examples describing both singly and doubly reinforced concrete simply supported beams subjected to a concentrated load, tested by Pera [17] and Alami and Ferguson [18] are presented in table 1, where we calculated the load – deflection diagrams.

	$E_s$ (MPa)	$f_y$ (MPa)	$E_c$ (MPa)	$f_c$ (MPa)	L(mm)	b(mm)	h(mm)
Beam tested by [17]	22E4	368	37600	41	500	20	50
Beam tested by [18]	2E5	342	34766	35	341.76	14.33	21.7

**Table 1:** Mechanical and geometrical properties of beams tested by Pera [17] and Alami and Ferguson [18].

Comparisons of the predictions of our model with these data are shown in figure 4, and figure 5. Material parameters corresponding to the shown curves are summarised in table 1. The values of the parameters needed in this model were those reported by these researchers. Figure 4 and figure 5 show the comparisons of the test results with the calculated results regarding load-deflection relationships.

In figure 4, experimental data and calculated results obtained by Alami and Ferguson [18] and those obtained by the present model are reported. As it can be seen from this figure, there is no difference between the present model and the one obtained from the experimental data. The effect of longitudinal reinforcement has not appeared. The longitudinal steel ratio in this case is smaller than that used in the case of the beam tested by Pera [17]. The present

model shows a slight increase in stiffness as compared to the results obtained by Merabet [19] (fig. 5). This increase of stiffness is the effect of the longitudinal reinforcement confinement.

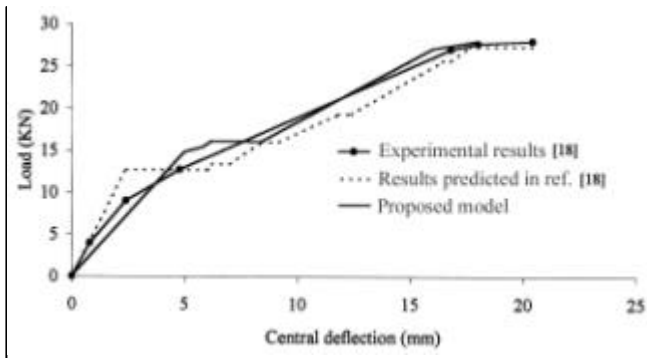


**Figure 4** Comparison of present model with deflection beam tested by Alami and Ferguson [18].

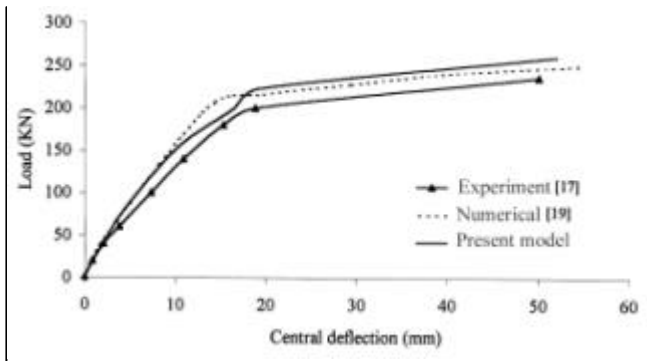


**Figure 5** Comparison of present model with deflection beam tested by Pera [17].

In figure 6, the plain line represents the results from the present model which take into account the longitudinal reinforcement effect on the ductility and strength of the concrete member. On the same figure, the results predicted by Kent and Park model [8] for compressive stress-strain curve are also shown. The descending branch of the curve presents a slight increase of ductility in our model. The increase of strength and ductility can be obviously attributed to the longitudinal reinforcement effect.

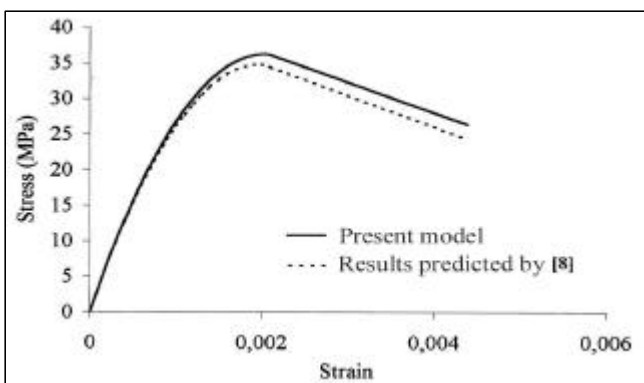


**Figure 6:** Comparison between the monotonic compressive stress-strain curve predicted by Kent and Park [8] and the proposed model.

## CONCLUSION

A model of confined reinforced concrete members is proposed. It takes into account the longitudinal reinforcement effect on the strength and ductility of members.

The comparison between the proposed model and the experimental results shows a good agreement between them and validates the present model. This model may trace the behaviour of reinforced concrete element up to the maximum load.

The change of the compressive stress-strain curve axis produced at the peak stress can be easily used to analyse the descending branch of the stress-strain curve.

## REFERENCES

- [1]- Leslie K.E., Rajagopalan S., Everard N.J., *ACI Journal Proceedings*, V.73, n°9 (1976), pp. 517-521.
- [2]- Tognon G., Ursella P., Coppetti G., *ACI Journal Proceedings*, V. 77, n°3 (1980), pp. 171-178.
- [3]- Watson S., *Journal of the Structural Division*, ASCE, 120, n°6 (1994), pp. 1798-1824.
- [4]- Légeron F. Paultre P., 4<sup>th</sup> international symposium on Utilization of High-strength /High-performance concrete, Paris (1996).
- [5]- Richart F.E., Brandtzaeg A., Brown R.L., University of Illinois Engineering Experimental Station, Bulletin n°190, (1929), 74 p.
- [6]- Balmer G.G., Structural Research Laboratory, Report n° SP-23, U. S. Bureau of reclamation, (1949), 13 p.
- [7]- Sargin M., Ghosh S.K., Handa V.K., *Magazine of concrete research*, V. 23, n°75-76, June-september (1971), pp. 99-110.
- [8]- Kent D.C. Park R., *Journal of the Structural Division*, ASCE, V. 97, ST 7, (1971), pp. 1969-1990.
- [9]- Pallewata J.M., Irawan P. and Maekawa K., *J. Materials, Conc. Struct., Pavements*, V. 28, n°520 (1995), pp. 297-308.
- [10]- Scott B.D., Park R., Priestley M.J.N., *ACI Journal Proceedings*, V. 79 (1982), pp. 13-27.
- [11]- Tetford T., "Comité Euro-International du béton, CEB – FIP, Model Code 1990", (1993), 457 p.
- [12]- Park R. Pauley T., "Reinforced concrete structures", John Wiley and Sons, (1975), 769 p.
- [13]- Shehata I.A.E.M., Shehata L.C.D., 4<sup>th</sup> International Symposium on Utilization of High-strength /High-performance concrete, Paris, (1996).
- [14]- Scanlon A., Murray D.W., *ASCE Journal of the structural division*, 100 (ST9), (1974), pp. 1911-1924.
- [15]- Cope R.J., Rao P.V., Clark L.A., CSCE-ASCE-ACI-CEB International Symposium, University of Waterloo, Ont., (1979), pp.379-407.
- [16]- Ahmed M.H., Ibrahim M.M.I., Mostafa, K.Z., Amin S.A., Third Arab Structural Engineering Conference, U.A. Emirates University, (1989), pp. 24-44.
- [17]- Pera J., These de Docteur – Ingénieur, INSA Lyon, (1973), 186 p.
- [18]- Alami Z.Y., Ferguson P.M., *ACI Journal Proceedings*, V.60, n°11 (1963), pp. 1643-1664.
- [19]- Merabet O., Thèse de Doctorat, INSA Lyon, (1990), 267 p.

□

